Progress In Electromagnetics Research, Vol. 141, 497–516, 2013

AZIMUTH MULTICHANNEL SAR IMAGING BASED ON COMPRESSED SENSING

Ming Jiang Wang[1, 2, *], Wei Dong Yu[1], and Robert Wang[1]

[1]Space Microwave Remote Sensing System Department, Institute of Electronics, Chinese Academy of Sciences, Beijing 100190, People's Republic of China

[2]Graduate University of the Chinese Academy of Sciences, Beijing 100090, People's Republic of China

Abstract—Azimuth multichannel is a promising technique of realizing high resolution and wide swath for synthetic aperture radar (SAR) imaging, which consequently leads to extremely high data rate on satellite downlink system and confronts serious ambiguity in subsequent processing due to its strict limitation of pulse repetition frequency (PRF). Ambiguity suppression performance of conventional spectrum construction is disappointing when the samples are approximately overlapped. To overcome these weaknesses, a novel sparse sampling scheme for displaced phase center antennas based on compressed sensing (CS) is proposed in this paper. The imaging strategy sparsely sampled in both range and azimuth direction, leading to a significant reduction of the system data amount beyond the Nyquist theorem, and then operated the CS technique in two dimensions to accomplish target reconstruction. Effectiveness of the proposed approach was validated through simulation and real data experiment. Simulation results and analysis indicated that the new imaging strategy could provide several favorable capability than conventional imaging algorithm such as less sampled data, better ambiguity suppression, higher resolution, and lower integrated sidelobe ratio (ISLR).

Received 22 May 2013, Accepted 20 July 2013, Scheduled 31 July 2013

* Corresponding author: Ming Jiang Wang (wangmingjiang.1987@163.com).

1. INTRODUCTION

Synthetic Aperture Radar (SAR) is an active remote sensing system which is widely utilized in many fields such as ocean surveillance, disaster monitoring, etc.. In these applications, a wide ground coverage and high azimuth resolution is always a primary preference for efficient use of the resources. However, in conventional SAR systems, high geometric resolution in azimuth and wide swath (HRWS) [1] coverage imposes contradicting requirements on system design: a high azimuth resolution requires a large Doppler bandwidth, which has to be sampled with a sufficiently high pulse repetition frequency (PRF). In contrast, the unambiguous swath width is directly related to the separation of subsequently transmitted pulses, meaning that a required swath width limits the PRF value [2]. Some classical operation modes have therefore been developed with different emphases on the trade-off. An effective solution for wide-swath imaging is ScanSAR [3, 4], which increases the unambiguous swath width at the cost of an impaired resolution, whereas spotlight mode [5, 6] can provide high resolution but with a limited coverage. To alleviate this conflict, an innovative idea called displaced phase center antenna (DPCA) [7] technique has been suggested in recent years. In DPCA, the system receives multiple pulses for every transmitted signal with multiple subapertures in along-track direction. This means that additional samples are gathered, thus increasing the effective sampling rates on receivers according to the number of subapertures. Consequently, either the resolution can be improved while the swath width remains constant, or the PRF can be reduced without rising azimuth ambiguities in this case. However, for DPCA system, traditional reconstruction method demands that the along-track displacement of receiving apertures to transmitting antenna and the system's operating PRF should fulfill strict conditions to provide a uniform effective azimuth phase. Any deviation of PRF could produce nonuniform sampling, leading to serious azimuth ambiguity if a matched filter is used directly, so further processing of the received signals is required before conventional monostatic SAR algorithms are applied. In [7, 8], a Doppler spectrum reconstruction method was proposed to suppressed the ambiguous energy caused by nonuniform sampling. The true spectrum is computed using the inverse of the joint frequency information matrices acquired from a combination of all of the channels. However, such a reconstruction is not robust when the samples are approximately overlapped. Another defection in DPCA system is that a sufficient sampling rate for range signal and a dense azimuth sampling are needed. The multichannel receivers will lead to huge data volume and bring a challenge not only to

the analog-to-digital (A/D) converter, but also to the on-board storage and downlink subsystem of satellite.

The recently introduced theory of compressed sensing (CS) [9, 10] is a new concept allowing the recovery of sparse signal that have been sampled below the traditional Nyquist sampling rate. In CS framework, it uses a low-dimensional nonadaptive, linear projection to acquire an efficient representation of a sparse signal with just a few measurements. Due to its compressed sampling ability, compressed sensing has found many attractions in radar remote sensing and branched out to many new fronts. R. Baraniuk et al. proposed the radar imaging system based on CS for the first time [11] and a high resolution imaging method is presented in [12] for SAR sparse targets reconstruction based on CS theory. Through using an overcomplete dictionary constructed by training samples, paper [13] introduced a new approach for SAR target classification based on Bayesian compressed sensing (BCS) and a novel sparse sampling scheme for high resolution wide swath spaceborne SAR based on CS theory was proposed in [14]. In the above researches, it has been shown that a successful recovery of a compressible signal depends on the presence of sparse dictionary and these works have made a great contribution to the future research of radar signal processing. However, as many of these approaches [15, 16] take traditional focusing with matched filtering in range direction and perform only azimuth focusing via CS, these methods cannot provide practical approaches to reduce the sampling rate of the receiver A/D converter.

This paper introduces a two-dimensional imaging algorithm for spaceborne DPCA SAR system based on compressed sensing through 2-D random sparse sampling. In the imaging scheme, a small proportion echoes are collected at a sub-Nyquist rate in azimuth direction among the multichannel receivers and each channel randomly samples fewer data in range direction, which can essentially mitigate the burden of the satellite data downlink system. Through sequently constructions of the measurement matrices in range and azimuth direction, the algorithm can accomplish an accurate recovery of the target scene with high resolution in a wide imaging swath utilized the CS technique. Unlike traditional matched filtering, it will be demonstrated that the proposed algorithm can reconstruct the targets with favorable azimuth ambiguity suppression performance and acquire a better imaging resolution under the circumstance of nonuniform sampling without any other further processing. In contrast to other compressive radar related algorithm that only considered using CS as part of one dimensional analog to information conversion, the developed method performs CS technique in both range and azimuth

dimensions. What's more important, the new CS imaging scheme can overcome the odd point barrier and remain a constant recovery whereas the traditional spectrum reconstruction method will lose its effectiveness when the multichannel sampling overlapped. The review paper is organized as follows. Section 2 gives a basic introduction of CS principle. In Section 3, we briefly reviewed the azimuth DPCA SAR systems. A two-dimensional sparse sampling scheme for DPCA system based on compressed sensing is analyzed and derived in Section 4. In Section 5, simulation and experiment results are presented to demonstrate the validity of the proposed method. Finally, discussions and conclusions are presented in Section 6.

2. COMPRESSED SENSING THEORY

Before going into further explanations about the scope of this paper, it is necessary to provide some background knowledge of compressed sensing. According the Shannon-Nyquist sampling theorem, a signal should be sampled with a frequency at least twice of its bandwidth to recovered the original signal exactly. However, the recently introduced compressed sensing theory states that it is available to reconstruct the sparse or compressible signals from only a small set of nonadaptive, linear measurements. It is said that according to CS, if properly chosen, the number of measurements can be much smaller than that of Nyquist rate samples [10] and the signal can be recovered with high probability when the measurement matrix satisfies certain condition. CS technique offers a framework of simultaneous sensing and compression of finite-dimensional vectors that relies on linear dimensionality reduction.

Suppose a finite length discrete-time signal vector $x \in C^I$ is K-sparse (if at most K of its coefficients are nonzero in a basis or more generally a frame $\Psi \in C^{I \times I}$), then the sparse signal can be expressed as:

$$x = \Psi\alpha \tag{1}$$

where $||\alpha||_0 = K \ll I$, $||\alpha||_0$ denotes l_0 norm and returns the number of nonzero elements of α. That is to say, vector x is a sparse representation of coefficient signal α in Ψ domain. Consider a $M \times I$ random measurement matrix $\Phi = [\phi_1, \phi_2, \ldots, \phi_I]$ with $M < I$ and ϕ_j, $j = 1, \ldots, I$ is a $M \times 1$ column vector,assuming M linear measurements of original signal are observed, then the measured signal $y \in C^M$ can be acquired through the following linear projections:

$$y = \Phi x = \Phi\Psi\alpha = \Theta\alpha \tag{2}$$

where $\Theta = \Phi\Psi$ is a $M \times I$ matrix. The matrix operation of measurement to signal x can be diagrammatized as in Figure 1.

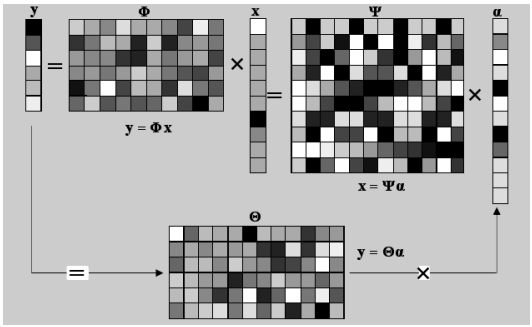

Figure 1. Matrix notation of measurement to signal x.

Since $M < I$, recovery of signal x from measurement y seems underdetermined and has infinitely many solutions. Nevertheless, according to CS theory, it can recover the sparse signal with high probability when the measurement matrix Θ satisfies the restricted isometry property (RIP) [17] which requires that:

$$(1 - \delta_k)||s||_2^2 \leq ||\Theta s||_2^2 \leq (1 + \delta_k)||s||_2^2 \tag{3}$$

where $\delta_k \in (0, 1)$, s is a column vector with a length of I. RIP condition can be essentially stated that all subsets of K columns taken from Θ are nearly orthogonal. A related condition, known as incoherence, requires that the rows of Φ cannot sparsely represent the columns of Ψ and vice versa. In fact, one can show that RIP can be achieved with high probability by simply selecting Φ as a random matrix [18].

A intuitive approach of recovering signal x from y can be concluded as solving the following l_0 minimization problem:

$$\hat{\alpha} = \arg\min ||\alpha||_0 \quad \text{s.t.} \quad y = \Phi\Psi\alpha = \Theta\alpha \tag{4}$$

unfortunately, although there are simple recovery conditions available, the above criterion is not reasonable in practice due to its NP-hard [19] limitation and sensitiveness to noise. In order to avoid these severe drawbacks, an alternative is to translate the l_0 minimization problem into something more tractable.According to the context of CS, it has been shown that the minimization of the l_0 problem is equivalent to the l_1 norm convex problem when the measurement matrix satisfies RIP condition and the recovery of sparse coefficients α can be achieved by seaching for the signal with a l_1 minimization criterion expressed as:

$$\hat{\alpha} = \arg\min ||\alpha||_1 \quad \text{s.t.} \quad y = \Theta\alpha \tag{5}$$

Some related researches also demonstrated that when Φ is chosen as Gaussian random matrix, the measurement matrix will have a small

restricted isometry constants δ_k and RIP holds with "a overwhelming probability" as long as $M = O(K \log(I/K))$ [20]. And then the original signal can be accurately recovered from the small set of M measurements through solving a l_1 norm minimization problem.

Computation of (5) is a convex optimization problem and can be solved using linear programming methods such as Basis Puisuit (BP) [21] technique. While Convex optimization techniques are powerful methods for computing sparse representations, there is a variety of greedy/iterative methods [22, 23] for solving such problems such as orthogonal matching pursuit (OMP) [24] and Iterative Hard Thresholding (IHT) [25] algorithm, etc.. As the greedy pursuit method are much faster and more efficient than other related algorithms, in this paper we mainly focus on OMP algorithm with the application to the recovery of sparse scene.

Figure 2 serves as an illustration of power of compressed sensing, which presents an example for the recovery of 3-sparse signal $x \in C^{128}$ from only 32 samples (denoted by the red circles in Figure 2(c)) using OMP algorithm. From the experiment result we can see that l_1 minimization performs an accurate recovery and the reconstructed spectrum is nearly identical to the spectrum truth. This illustration vividly shows us that the CS sampling scheme has the the potential to reduce the sampling data amount and OMP algorithm is qualified to

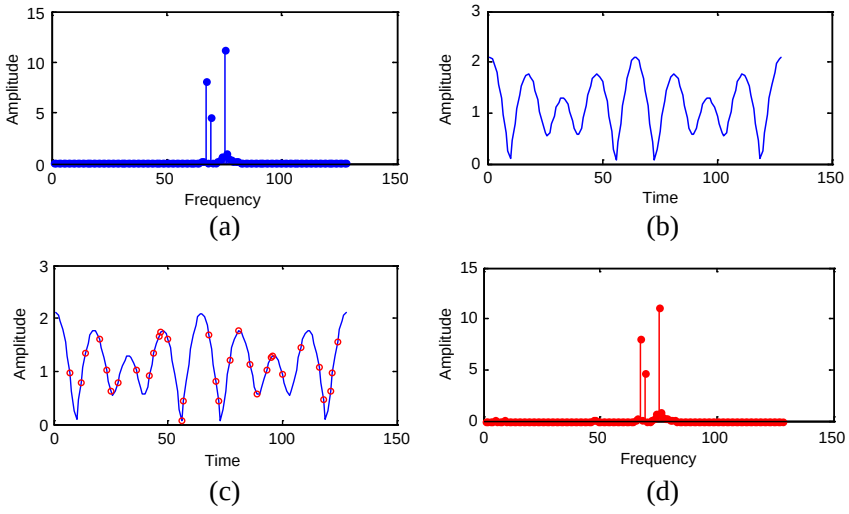

Figure 2. (a) 3-sparse Fourier spectrum. (b) 128 Nyquist sampling of time domain signal. (c) 32 compressed random samplings of the time domain signal with length 128. (d) Spectrum reconstruction via l_1 minimization.

guarantee an accurate recovery for sparse signal under the compressive sampling situation.

3. AZIMUTH MULTICHANNEL SAR IMAGING MODEL

Azimuth multichannel technique is an innovative approach to achieve high resolution and wide swath SAR imaging. Figure 3 shows one example for displaced phase center antenna imaging scenario, where a single centered subantenna transmits waveform to illuminate a wide swath and N subapertures along-track simultaneously record the scattered signal from the illuminated footprint. d_{az} is the length of subaperture and Vs is the velocity of the SAR platform. In an ideal situation, it will allow for a reduction of the pulse repetition frequency (PRF) by a factor of N without rising azimuth ambiguities, which is beneficial to acquire a wide ground coverage for the imaging system. This reduction of the azimuth sampling rate becomes possible by a coherent combination of each individual receiving signal where the ambiguous parts of the Doppler spectra cancel each other. For optimum performance, the along-track displacement between two adjacent equivalent phase centers should be chosen as:

$$d = \frac{2Vs}{N \cdot \mathrm{PRF}} \tag{6}$$

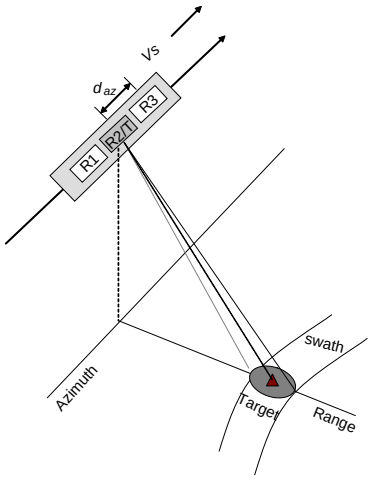

Figure 3. Imaging geometry model of spaceborne DPCA SAR.

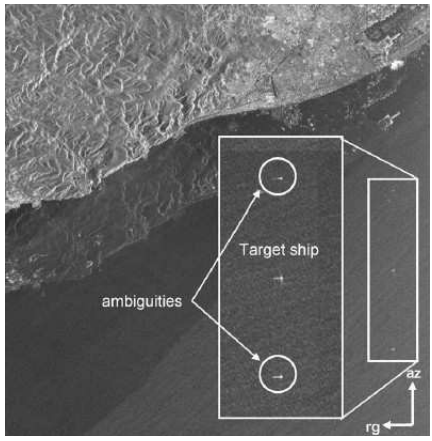

Figure 4. Imaging with nonuniform sampling data of TerraSAR-X.

which will generate a uniform sampling of the received azimuth signal and a simple arrangement of the samples from the subapertures can be focused using algorithms designed for monochannel SAR, such as the range Doppler algorithm (RDA). Since the subaperture distance and the platform velocity are fixed in practical system, a specific PRF will be required according to Equation (6) so that the SAR platform moves just one half of the total antenna length between subsequent radar pulses. Nevertheless, such a rigid selection of PRF may be in conflict with the timing diagram for some incident angles, which excludes the opportunity to use an increased PRF for improved azimuth ambiguity suppression. Obviously, such a rigid persistence is difficult for many real cases and any deviation of the PRF will lead to nonuniform sampling and an incorrect focus if using a matched filter directly.

Figure 4 presents a specific illustration of imaging ambiguities for a ship target near the Bercelona coast caused by nonuniform sampling in TerraSAR-X [26] (which is equipped with the split dual antennas allowing the simultaneous acquisition of reflected signals from targets). According to the parameter listed in [27], the separation between two successive spatial samples for the uniform sampling mode of the system corresponding to 1.2 m. However, the system operating PRF for this imaging data is 3.773 kHz, leading to a separation of 0.827 m between successive sample pairs and a strong nonuniformity. The focus of the nonuniform sampling data without preprocessing was shown in Figure 4 and significant ambiguities of ship target can be observed from the incorrect focusing image, which can introduce serious disturbance for the ship detection.

Due to the serious ambiguities introduced by nonuniform sampling, further processing of the azimuth multichannel signals is required before conventional monostatic SAR imaging algorithms are applied. In paper [28], an unambiguous spectrum reconstruction algorithm is derived for nonuniform sampling of SAR signal. However, since the true spectrum was computed using the inverse of the joint frequency information matrices acquired from a combination of all of the channels, such a reconstruction does not perform robust when the samples overlapped each other. In this paper, we presented a more efficient two-dimensional imaging scheme based on CS for azimuth multichannel system without other preprocessing even for serious nonuniform sampling through the combination of signal analysis in DPCA and sparse modeling in compressed sensing. Besides, what need to be highlighted for the proposed method is that it can accomplish a stable recovery regardless of wether the PRF is operating at a singular point.

4. AZIMUTH MULTICHANNEL SAR IMAGING BASED ON COMPRESSED SENSING

Figure 3 illustrated the imaging geometry of stripmap mode azimuth multichannel SAR and how the echo was sampled: the center antenna transmits radar pulses and the backscattered energy from illuminated target located at $\Gamma(t', \tau') \in \Omega$ is received simultaneously by N subantennas. Suppose the transmitting waveform is a chirp signal expressed as:

$$s_T(\tau) = \text{rect}\left(\frac{\tau}{T_r}\right) \exp\left(j\pi K_r \tau^2\right), \tag{7}$$

where $\text{rect}(\cdot)$ is a unit rectangular window, τ the range fast time, T_r the duration of the transmitted pulse, and K_r the chirp rate. For the ith receiving antenna separated with the transmitting antenna by distance $d_i = (i - \frac{N+1}{2}) \cdot d_{az}$, $i = 1, \ldots, N$, the actual received signal of channel i can be represented as:

$$\begin{aligned} s_i(t, \tau) = & \iint\limits_{\Gamma \in \Omega} \sigma'(t', \tau') \cdot \text{rect}\left\{\frac{\tau - R_i(t - t', \tau')}{T_r}\right\} \\ & \cdot \text{rect}\left\{\frac{t - t'}{T_a}\right\} \cdot \exp\left(-j2\pi f_0 R_i\left(t - t', \tau'\right)/c\right) \\ & \exp\left(j\pi K_r \left(\tau - R_i(t - t', \tau')/c\right)^2\right) dt' d\tau', \quad i = 1, \ldots, N. \end{aligned} \tag{8}$$

and the slant range of channel i can be defined by

$$R_i\left(t - t', \tau'\right) = \sqrt{\left(\frac{\tau' c}{2}\right)^2 + \left[v_a(t - t')\right]^2} + \sqrt{\left(\frac{\tau' c}{2}\right)^2 + \left[v_a(t - t') + d_i\right]^2} \tag{9}$$

where c is the velocity of the electromagnetic wave propagation in free space, $\sigma'(t', \tau')$ the reflectivity of the point target $\Gamma(t', \tau')$, t the azimuth slow time, T_a the synthesis aperture time, and f_0 the carrier frequency. $R_i(t - t', \tau')$ is instantaneous slant range from the transmitting antenna to the target and back to the i-th receiving antenna.

4.1. Range Recovery Based on CS

Consider the target scene reflectivity was discretized and generated with $t' = m\Delta t'$, $m = 1, \ldots, N \cdot N_a$, $\Delta t' = \frac{1}{N \cdot \text{PRF}}$, $\tau' = n\Delta\tau'$, $n = 1, \ldots, N_r$, $\Delta\tau' = \frac{1}{F_r}$, $N \cdot N_a$ and N_r are azimuth and range length of the observed scene, F_r is the range sample frequency, then the signal

of channel i can be written as:

$$\begin{aligned} s_i(t,\tau) &= \sum_{m=1}^{N\cdot N_a}\sum_{n=1}^{N_r}\sigma(m,n)\cdot \mathrm{rect}\left\{\frac{\tau - R_i(t-m\Delta t', n\Delta\tau')}{T_r}\right\}\cdot \mathrm{rect}\left\{\frac{t-m\Delta t'}{T_a}\right\} \\ &\quad \cdot \exp\left(-j2\pi f_0 R_i\left(t-m\Delta t', n\Delta\tau'\right)/c\right)\cdot \exp\left(j\pi\left(\tau - R_i(t-m\Delta t', n\Delta\tau')/c\right)^2\right) \\ &= \sum_{n=1}^{N_r}\left\{\sum_{m=1}^{N\cdot N_a}\sigma(m,n)\cdot \mathrm{rect}\left(\frac{t-m\Delta t'}{T_a}\right)\cdot \exp\left(-j2\pi f_0 R_i\left(t-m\Delta t', n\Delta\tau'\right)/c\right)\right\} \\ &\quad \cdot \mathrm{rect}\left\{\frac{\tau - R_i(t-m\Delta t', n\Delta\tau')}{T_r}\right\}\cdot \exp\left\{j\pi\left[\tau - R_i\left(t-m\Delta t', n\Delta\tau'\right)/c\right]^2\right\}, \\ &\quad i = 1,\ldots,N. \end{aligned} \tag{10}$$

where $\sigma(m,n) = \sigma'(m\Delta t', n\Delta\tau')$. At a given azimuth time t_0, if we note that:

$$\sigma_r(n) = \sum_{m=1}^{N\cdot N_a}\sigma(m,n)\cdot rect\left(\frac{t_0 - m\Delta t'}{T_a}\right)\cdot \exp\left(-j2\pi f_0 R_i\left(t_0 - m\Delta t', n\Delta\tau'\right)/c\right)$$

then the range signal at azimuth time $t = t_0$ can be represented as a linear superposition of the delay sequence of transmitted signal $s(\tau)$ and Equation (10) can be expressed as:

$$\begin{aligned} & s_i(\tau)|_{t=t_0} = s_i(t_0,\tau) \\ &= \sum_{n=1}^{N_r}\sigma_r(n)\cdot \mathrm{rect}\left\{\frac{\tau - R_i(t_0 - m\Delta t', n\Delta\tau')}{T_r}\right\} \\ &\quad \cdot \exp\left\{j\pi\left[\tau - R_i(t_0 - m\Delta t', n\Delta\tau')/c\right]^2\right\}, \quad i = 1,\ldots,N \end{aligned} \tag{11}$$

if we sample the received range signal $s_i(\tau)$ not at every interval $\Delta\tau$ but at a random time sequence $\omega(p)\cdot\Delta\tau$, where $\Delta\tau = \Delta\tau' = \frac{1}{F_r}$, $\omega(p)$ is a $1\times P$ random sequence, then P samples of the range signal can be obtained:

$$\begin{aligned} S_i(p) &= s_i(\omega(p)\cdot\Delta\tau)|_{t=t_0} \\ &= \sum_{n=1}^{N_r}\sigma_r(n)\cdot \mathrm{rect}\left\{\frac{\omega(p)\cdot\Delta\tau - R_i(t_0 - m\Delta t', n\Delta\tau')}{T_r}\right\} \\ &\quad \cdot \exp\left(j\pi\left(\omega(p)\cdot\Delta\tau - R_i(t_0 - m\Delta t', n\Delta\tau')/c\right)^2\right), \quad p = 1,\ldots,P \end{aligned} \tag{12}$$

According to CS theory, when the range signal $s_i(\tau)|_{t=t_0}$ is sparse ($\sigma_r(n)$ has only a few nonzero elements), the low rate samples $S_i(p)$ contained sufficient information to reconstruct the signal $\sigma_r(n)$ corresponding to the Nyquist-rate samples of the scene reflectivity. At

this point, the measurement matrix $\Phi_r \in C^{P\times N_r}$ for range dimension can be constructed through Equation (12) and expressed as:

$$\begin{aligned}\Phi_r(p,q) &= s_T\left((\omega(p)-q)\cdot\Delta\tau\right)\\ &= \text{rect}\left[\frac{(\omega(p)-q)\cdot\Delta\tau}{T_r}\right]\exp\left[j\pi K_r\left((\omega(p)-q)\cdot\Delta\tau\right)^2\right] \quad (13)\end{aligned}$$

when the CS frame was built, the reconstruction of range profile can be recovered by solving a convex optimization problem through OMP algorithm.

4.2. Azimuth Processing Based on CS

After range compression, the azimuth signal of channel i at a given range gate $\tau_0 = p_0\Delta\tau$ can be approximated as:

$$\begin{aligned}s_i(t,p_0\Delta\tau) &= \sum_{m=1}^{N\cdot N_a}\sigma(m,n)\cdot\text{rect}\left(\frac{t-m\Delta t'}{T_a}\right)\cdot\exp\left(-j2\pi f_0 R_i(t-m\Delta t',n\Delta\tau')/c\right)\\ &\quad\cdot\delta\left(p_0\Delta\tau - R_i(t-m\Delta t',n\Delta\tau')/c\right)\\ &\approx \sum_{m=1}^{N\cdot N_a}\sigma(m,n_0)\cdot\text{rect}\left(\frac{t-m\Delta t'}{T_a}\right)\\ &\quad\cdot\exp\left(-j2\pi f_0 R_i(t-m\Delta t',n_0\Delta\tau')/c\right), \quad i=1,\ldots,N \quad (14)\end{aligned}$$

where $\delta(\cdot)$ is *Dirac function* and $p_0\Delta\tau \cong R_i(t-m\Delta t',n_0\Delta\tau')/c$. Similarly, in our sparse sampling scheme, supposing the centered antenna transmits radar pulses at a random pulse repetition interval $\omega(k)\Delta t$ rather than a regular interval Δt, where $\Delta t = \frac{1}{\text{PRF}} = N\cdot\Delta t'$, then the azimuth observed signal of channel i for range gate τ_0 can be written as:

$$\begin{aligned}y_i(k) &= s_i\left(\omega(k)\Delta t,\tau\right)|_{\tau=\tau_0}\\ &= \sum_{m=1}^{N\cdot N_a}\sigma(m,n_0)\cdot\text{rect}\left(\frac{\omega(k)\Delta t - m\Delta t'}{T_a}\right)\\ &\quad\cdot\exp\left(-j2\pi f_0 R_i(\omega(k)\Delta t - m\Delta t',n_0\Delta\tau')/c\right)\\ &= \sum_{m=1}^{N\cdot N_a}\sigma(m,n_0)\cdot\text{rect}\left(\frac{\omega(k)\cdot N\Delta t' - m\Delta t'}{T_a}\right)\\ &\quad\cdot\exp\left(-j2\pi f_0 R_i\left(\omega(k)\cdot N\Delta t' - m\Delta t',n_0\Delta\tau'\right)/c\right) \quad i=1,\ldots,N \quad (15)\end{aligned}$$

and the azimuth measurement matrix $\Phi_{ai} \in C^{K\times N\cdot N_a}$ for channel i can be concluded as:

$$\Phi_{ai}(k,l) = \text{rect}\left[\frac{(\omega(k)\cdot N - l)\,\Delta t'}{T_a}\right] \cdot \exp\left(-j2\pi f_0 R_i\left(\left(\omega(k)\cdot N - l\right)\Delta t', n_0\Delta\tau'\right)/c\right) \quad i = 1,\ldots,N \tag{16}$$

where $k = 1,\ldots,K \cdot l = 1,\ldots,N\cdot N_a$, K is the number of random transmitted pulses sequence, so the azimuth observed model for channel i at range gate n_0 can be presented as:

$$y_i(k) = \Phi_{ai}^{(k)} \cdot \sigma_{n_0} \tag{17}$$

$\Phi_{ai}^{(k)}$ denotes the k-th row of matrix Φ_{ai} and σ_{n_0} is a $1\times N\cdot N_a$ vector which denotes the azimuth reflectivity at range gate n_0. According to the theory of DPCA, the total azimuth observed signal can be illustrated as:

$$Y = [y_1(1) \quad \ldots \quad y_N(1) \quad \ldots \quad y_1(K) \quad \ldots \quad y_N(K)]^T \tag{18}$$

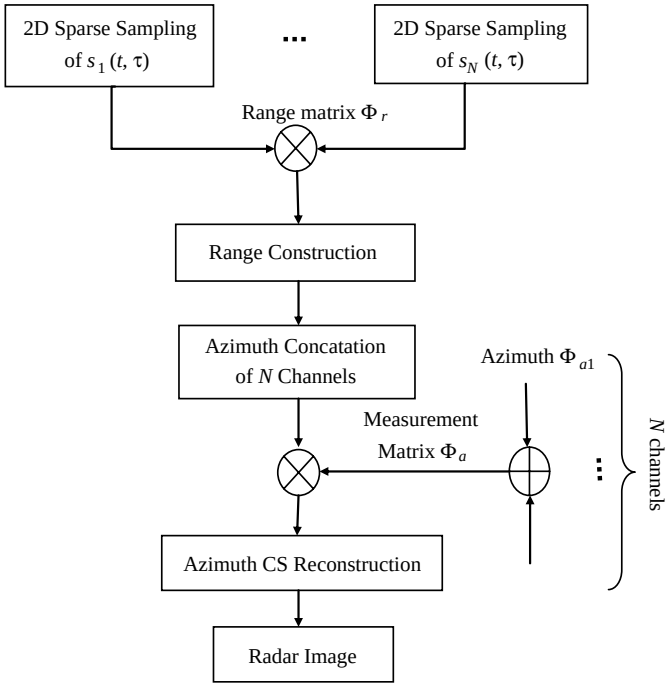

Figure 5. Flowchart of azimuth multichannel SAR imaging algorithm based on compressed sensing.

$[\cdot]^T$ means the transposition of matrix. Then the realization of the total azimuth measurement matrix $\Phi_a \in C^{N\cdot K\times N\cdot N_a}$ for the DPCA system can be accomplished through corresponding rearrangement of all the sub measurement matrixes Φ_{ai}:

$$\Phi_a = \left[\Phi_{a1}^{(1)} \quad \cdots \quad \Phi_{aN}^{(1)} \quad \cdots \quad \Phi_{a1}^{(K)} \quad \cdots \quad \Phi_{aN}^{(K)}\right]^T \tag{19}$$

and the azimuth observed model at range gate n_0 can be signified as:

$$Y_{n_0} = \Phi_a \sigma_{n_0} \tag{20}$$

method ibid: the solution of Equation (20) can be obtained by solving a l_1 minimization problem as Equation (5) through OMP algorithm and finally we can get the two-dimensional radar image of the scene. The whole processing flowchart of the two dimensional DPCA SAR imaging algorithm based on CS can be diagrammed as Figure 5.

5. EXPERIMENTAL RESULTS

In this section, simulation and real data experiment will be processed and analyzed to validate the effectiveness of the proposed method for azimuth multichannel SAR imaging through comparison with traditional processing technique.

5.1. Simulation Results

To evaluate the performance of proposed CS based method, we consider a point target located at Γ (0 m, 700 km) with unit magnitude to generate the echoes in the first example. The detailed parameters of the system are listed in Table 1.

According to the parameter table, the total length of azimuth antenna is 12.6 m, and three subarrays are uniformly divided. The center subantenna transmits signal with a bandwidth of 66.4 MHz and all subapertures receive the back waveform. The Doppler bandwidth is near 3600 Hz with a corresponding azimuth resolution of 2.08 m and the PRF is set to 1500 Hz yielding a highly nonuniform sampling. Echoes of the target were generated separately through traditional Nyquist sampling based on Equation (10) and 3×3 times sparse random undersampling based on CS scheme. Results of the target reconstruction through traditional RD algorithm and CS based method were shown in Figure 6.

Comparing Figures 6(a) and (b), we can see that the CS based method can accurately reconstruct the point target with only a few samples of the echo, whereas severe ambiguities appear at (-1200 m, 700 km) and (1200 m, 700 km) in the conventional RD imaging due to

Table 1. System parameters for the simulation experiment.

Azimuth subaperture number N	**3**
Wavelength λ	0.03 m
Altitude H	495 km
Slant range R	700 km
Antenna length L	12.6 m
Bandwidth B_r	66.4 MHz
Subaperture Length d_{az}	4.15 m
Pulse width T_r	5 μs
Platform velocity V_s	7500 m/s
Pulse repeat frequency (PRF)	1500 Hz
Incidence angle θ	45 deg
Range undersampling	3 times
Azimuth undersampling	3 times

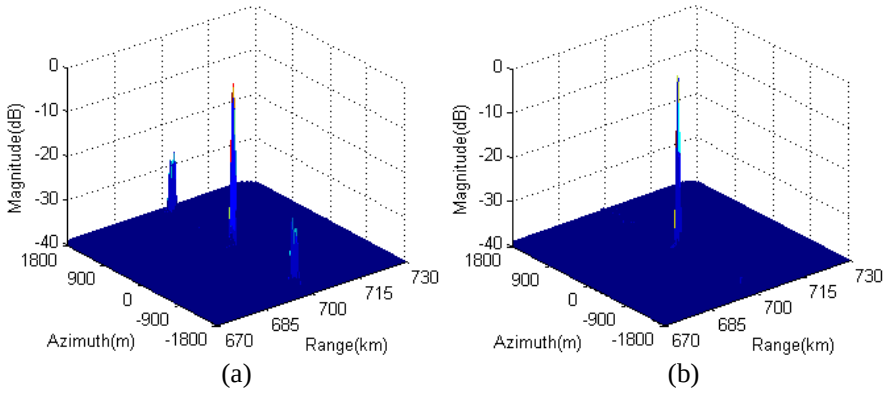

Figure 6. Target recovery of nonuniform sampling. (a) RD imaging with full samples without spectrum reconstruction. (b) CS based recovery with 11.1% samples.

its spectrum aliasing. Generally, the ambiguities caused by nonuniform sampling can be suppressed by Doppler spectrum reconstruction method [7]. However, the filtering method is not robust when the system working PRF approximates $\frac{2 \cdot V_s}{i \cdot d_{az}}$, $i = 1, \ldots, N-1$, which corresponding to an overlapping samples scheme. Illustration of this point is shown in Figure 7 when the selection of PRF is close to

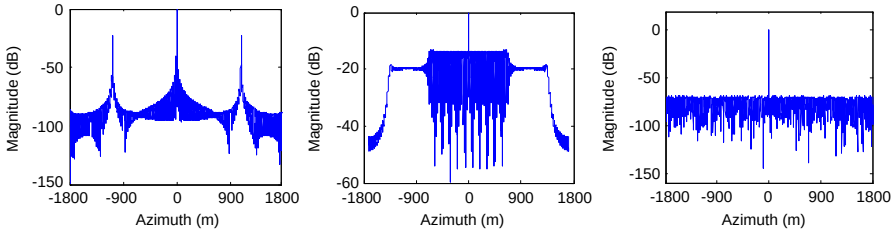

Figure 7. Azimuth profile of target reconstruction with different method (PRF $\approx$ 1800 Hz). (a) RD imaging with full samples before spectrum reconstruction. (b) RD imaging with full samples after spectrum reconstruction. (c) CS based recovery with 30% samples.

1800 Hz. From Figure 7 we can see that when the samples are nearly overlapped, the spectrum reconstruction method performance is disappointing with an elevation of ambiguity energy to nearly -15 dB, whereas the CS based algorithm can constantly accomplish an accurate recovery regardless of the deviation of PRF.

Analysis above convictively shows the advantage of the new method that it can elimate the ambiguity raised by the nonuniform sampling and accurately focus all the back scattered energy to the target point. The main explanation for this wonderful speciality may be interpreted as that through nonadaptive and linear measurement, CS scheme is not sensitive to the nonuniformity of the sampling. Thus, the CS based method can remove the disturbance of nonuniform sampling and accomplish an exact recovery of the target regardless of whether the sampling data is uniform or not.

5.2. Super Resolution and ISLR Analysis

Besides the advantage mentioned above, another notable superiority of the proposed method is its lower Integrated Side Lobe Ratio (ISLR) and super resolution compared with traditional imaging algorithm. Quantitative imaging capacity evaluations of both methods (CS based reconstruction and matched filter imaging) are listed in Table 2, which indicates that the ISLR of the target recovered from the new method is lower and the CS based imaging scheme can reconstruct more details beyond the conventional theoretical limitation. To confirm this specialty, a further experiment is carried out using parameters in Table 1. Two points targets T_1 (0 m, 700 km) and T_2 (2 m, 700 km) are located at different azimuth distances and 2 meters apart. In this case, the conventional imaging method cannot distinguish the two

Table 2. Evaluations of the azimuth resolution and ISLR.

		PRF (Hz)				
		1000	1100	1200	1300	1400
Aizmuth Resolution (m)	MF	2.212	2.119	2.040	2.062	2.081
	CS	1.846	1.828	1.825	1.837	1.843
Azimuth ISLR (dB)	MF	−17.83	−18.15	18.29	−18.20	−18.07
	CS	−19.10	−19.17	−19.26	−19.24	−19.22

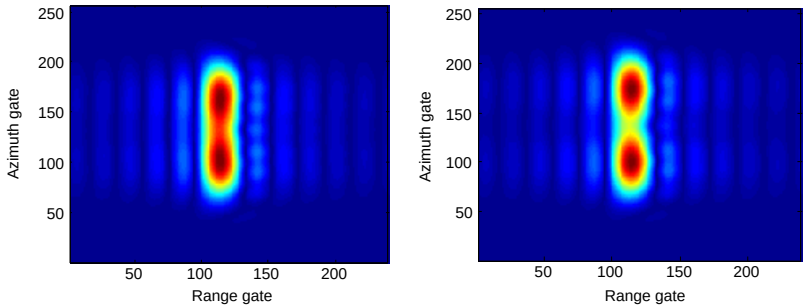

Figure 8. Contour of two targets T_1 and T_2 with both method. (a) RD imaging. (b) CS based recovery.

point targets as shown in Figure 8(a) due to their spacing is less than theoretical resolution. Conversely, the proposed CS based method can make an evident distinction between targets T_1 and T_2 after 16 times interpolation illustrates as in Figure 8(b). The illustration indicates that the new imaging algorithm is conductive for the improvement of imaging resolution.

5.3. Real Data Processing Results

The new algorithm has also been investigated with a block of real SAR data containing two ships in the ocean acquired by the RADARSAT-1 [3] system (see the yellow rectangle in Figure 9(a)). Since there is no multichannel mode in the RADARSAT-1 system, monostatic data were used in the example. The raw data, which have been originally sampled at a frequency f_a in azimuth, were filtered with an ideal low pass filter of bandwidth $B = f_a/3$ to get the SAR data oversampled by a factor of 3. Then, the ambiguous inputs to the

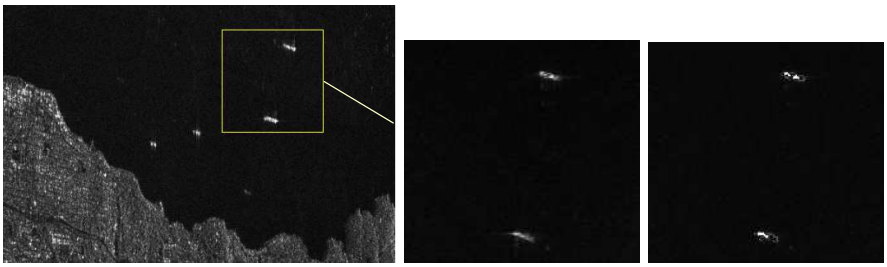

Figure 9. Imaging of original Radrasat-1 raw data with different methods: (a) Original radarsat-1image with two distributed ships targets. (b) RD imaging with full samples and uniform sampling. (c) CS based recovery with 11.1% samples after nonuniform processing.

three azimuth multichannel have been formed by taking every 9th sample for each channel. Selecting adjacent samples for the three channels will result in a maximum nonuniform sampling, while a distance of three samples will generate a uniform sampling. After the nonuniform sampling processing completed, the CS sampling scheme follows with a 3×3 times downsampling in range and azimuth, respectively. Figures 9(b) and (c) compare the experiment results of RD imaging with the full uniform sampling and the CS recovery under a maximum of nonuniform sampling condition with only a few set of the samples. From the experimental results we can see that the new algorithm can complete an exact reconstruction of the ship targets as expected and there is not much difference between the imagings of two methods. Although sparse sampling of CS may lead to some energy loss for the imaging magnitude, the targets in the imaging are discernable and experimental result is acceptable. This illustration demonstrates that the new method is well applicative to the realities and efficient for the real sparse cases.

6. DISCUSSIONS AND CONCLUSIONS

An innovative algorithm for azimuth multichannel SAR imaging based on CS in derived in this paper. In the new imaging scheme, radar system randomly transmits fewer pulses in azimuth and samples fewer data in range than traditional system. Through constructing measurement matrixes in range and azimuth sequently, the algorithm applies the CS technique in two dimensions with a significant reduction of data amount. Several favorable capacities of the algorithm have been

demonstrated in this paper such as super resolution, lower ISLR and better ambiguity suppression in case of nonuniform sampling, thereby avoiding the stringent restriction of PRF. The innovative imaging plan can find great potential in the application of currently azimuth displaced phase center antenna systems like HRWS or dual receive antennas approaches in TerraSAR-X and Radarsat-2 [29], especially appropriate for the instance when the imaging scene is sparse, such as ships detection and ocean imaging. Effectiveness of the algorithm has been proved by simulation experiments and it is indicated that the proposed algorithm is not only efficient in sampling data reduction, but also profitable for the quality elevation of imaging in nonuniform sampling scheme. What need to be mentioned is that the CS based imaging algorithm is equipped with the excellent ambiguity suppression performance at the cost of increase in computational load. In addition, the CS recovery scheme is susceptible to noises and sparseness of the observed area. When the system is situated in a drastic noisy environment and the target scene does not meet the sparse requirement, the recovery performance may not seem so good and suffers a depression of the imaging capacity. Thus, further efforts should be focused on finding a solution of the weakness mentioned above and how to apply this technique to practical systems is also up in the air and need to be further explored.

REFERENCES

1. Xu, W., P. P. Huang, and Y. K. Deng, "Multi-channel SPCMB-TOPS SAR for high resolution wide-swath imaging," *Progress In Electromagnetics Research*, Vol. 116, 533–551, 2011.
2. Gebert, N., G. Krieger, and A. Moreira, "Multichannel azimuth processing in ScanSAR and TOPS mode operation," *IEEE Trans. Geosci. Remote Sensing*, Vol. 48, No. 7, 2994–3008, 2010.
3. Cumming, I. G. and F. H. Wong, *Digital Processing of Synthetic Aperture Radar Data: Algorithms and Implementation,* Publishing House of Electronics Industry, 2007.
4. Huang, P., W. Xu, and W. Qi, "Two dimension digital beamforming preprocessing in multibeam scan SAR," *Progress In Electromagnetics Research*, Vol. 136, 495–508, 2013.
5. Carrara, W., R. Goodman, and R. Majewski, *Spotlight Synthetic Aperture Radar: Signal Processing Algorithm,* Artech House, Boston, 1995.
6. Guo, D. M., H. P. Xu, and J. W. Li, "Extended wavenumber domain algorithm for highly squinted sliding spotlight SAR data

processing," *Progress In Electromagnetics Research*, Vol. 114, 17–32, 2011.

7. Gebert, N., *Multi-channel Azimuth Processing for High-resolution Wide-swath SAR Imaging,* DLR, Bibliotheks und Informationswesen, 2009.
8. Jenq, Y.-C., "Perfect reconstruction of digital spectrum from nonuniformly sampled signals," *IEEE Transactions on Instrumentation and Measurement*, Vol. 46, No. 3, 649–652, 1997.
9. Donoho, D., "Compressed sensing," *IEEE Trans. Inf. Theory*, Vol. 52, No. 4, 1289–1306, 2006.
10. Candès, E., J. Romberg, and T. Tao, "Robust uncertainty principles: Exact signal reconstruction from highly incomplete frequency information," *IEEE Trans. Inf. Theory*, Vol. 52, No. 2, 489–509, 2006.
11. Baraniuk, R. and P. Steeghs, "Compressive radar imaging," *Proc. IEEE Radar Conf.*, 128–133, Waltham, MA, Apr. 2007.
12. Wei, S. J., X. L. Zhang, J. Shi, and G. Xiang, "Sparse reconstruction for SAR imaging based on compressed sensing," *Progress In Electromagnetics Research*, Vol. 109, 63–81, 2010.
13. Zhang, X., J. Qin, and G. Li, "SAR target classification using Bayesian compressive sensing with scattering centers features," *Progress In Electromagnetics Research*, Vol. 136, 385–407, 2013.
14. Chen, J., J. H. Gao, Y. Q. Zhu, W. Yang, and P. B. Wang, "A novel image formation algorithm for high-resolution wide-swath spaceborne SAR using compressed sensing on azimuth displacement phase center antenna," *Progress In Electromagnetics Research*, Vol. 125, 527–542, 2012.
15. Zhang, L., M. D. Xing, C. W. Qiu, et al., "Achieving higher resolution ISAR imaging with limited pulses via compressed sensing in sparse aperture imaging of radar," *IEEE Geosci. Remote Sens. Lett.*, Vol. 6, No. 3, 567–571, 2009.
16. Alonso, M. T., P. Lopez-Dekker, and J. J. Mallorqui, "A novel strategy for radar imaging based on compressive sensing," *IEEE Geosci. Remote Sens. Lett.*, Vol. 42, No. 18, 4285–4295, 2010.
17. Baraniuk, R., "Compressive sensing," *IEEE Signal Process.*, Vol. 24, No. 4, 118–121, 2007.
18. Candès, E., "Compressive sampling," *Proc. Int. Congr. Math.*, Vol. 3, 1433–1452, 2006.
19. Candes, J., "The restricted isometry property and its implications for compressed sensing," *Comptes Rendus Mathematique*, Vol. 346, No. 9, 589–592, Paris, 2008.

20. Candès, E., J. Romberg, and T. Tao, "Stable signal recovery from incomplete and inaccurate measurements," *Commun. Pure Appl. Math.*, Vol. 59, No. 8, 1207–1223, 2006.
21. Chen, S., D. Donoho, and M. Saunders, "Atomic decomposition by basis pursuit," *SIAM Rev.*, Vol. 43, No. 1, 129–159, 1998.
22. Eldar, Y. C. and G. Kutyniok, *Compressed Sensing: Theory and Applications,* Cambridge University Press, 2012.
23. Davis, G., S. Mallat, and M. Avellaneda, "Adaptive greedy approximations," *Constr. Approx.*, Vol. 13, No. 1, 57–98, 1997.
24. Tropp, J. and A. Gilbert, "Signal recovery from random measurements via orthogonal matching pursuit," *IEEE Trans. Inf. Theory*, Vol. 53, No. 12, 4655–4666, 2007.
25. Blumensath, T. and M. Davies, "Iterative hard thresholding for comressive sensing," *Appl. Comput. Harmon. Anal.*, Vol. 27, No. 3, 265–274, 2009.
26. Brusch, S., S. Lehner, T. Fritz, M. Soccorsi, A. Soloviev, and B. van Schie, "Ship surveillance with TerraSAR-X," *IEEE Trans. Geosci. Remote Sensing*, Vol. 49, No. 3, 1092–1103, 2011.
27. Kim, J.-H., M. Younis, P. Prats-Iraola, M. Gabele, and G. Krieger, "First spaceborne demonstration of digital beamforming for azimuth ambiguity suppression," *IEEE Trans. Geosci. Remote Sensing*, Vol. 51, No. 1, 579–590, 2013.
28. Krieger, G., N. Gebert, and A. Moreira, "Unambiguous SAR signal reconstruction from nonuniform displaced phase center sampling," *IEEE Geosci. Remote Sens. Lett.*, Vol. 1, No. 4, 260–264, 2004.
29. Brule, L. and H. Baeggli, "Radarsat-2 program update," *Proc. IGARSS*, Vol. 2, 1186–1189, 2002.